Dalton Transactions

Accepted Manuscript

This article can be cited before page numbers have been issued, to do this please use: Q. Zhang, X. Chen, J. Chen, X. Wu, R. Yu and C. Lu, *Dalton Trans.*, 2015, DOI: 10.1039/C5DT01108F.

This is an *Accepted Manuscript*, which has been through the Royal Society of Chemistry peer review process and has been accepted for publication.

Accepted Manuscripts are published online shortly after acceptance, before technical editing, formatting and proof reading. Using this free service, authors can make their results available to the community, in citable form, before we publish the edited article. We will replace this *Accepted Manuscript* with the edited and formatted *Advance Article* as soon as it is available.

You can find more information about *Accepted Manuscripts* in the Information for Authors.

Please note that technical editing may introduce minor changes to the text and/or graphics, which may alter content. The journal's standard Terms & Conditions and the Ethical guidelines still apply. In no event shall the Royal Society of Chemistry be held responsible for any errors or omissions in this *Accepted Manuscript* or any consequences arising from the use of any information it contains.

ROYAL SOCIETY OF CHEMISTRY

www.rsc.org/dalton

Dalton Transactions

Dynamic Article Links ►
View Article Online
DOI: 10.1039/C5DT01108F

Cite this: DOI: 10.1039/c0xx00000x

www.rsc.org/xxxxxx

ARTICLE TYPE

Photo- and Electro-luminescence of four cuprous complexes with Sterically Demanding and Hole Transmitting Diimine Ligands

Qing Zhang,[a,b,c] Xu-Lin Chen,[a,b] Jun Chen,[c] Xiao-Yuan Wu,[a,b] Rongmin Yu,[*,a,b] and Can-Zhong Lu [*,a,b]

Received (in XXX, XXX) Xth XXXXXXXXX 20XX, Accepted Xth XXXXXXXXX 20XX

DOI: 10.1039/b000000x

Four new cuprous complexes (**1**–**4**) containing bisphosphine and triazolylpyridine donors have been prepared in order to examine the effect of methyl group and carbazole appendage on photo- and electro-luminescent (PL and EL) properties. Because of their additional steric hindrance from methyl substituent group at 6-pyridine ring, complexes **3** and **4**, compared with the methyl group free compounds **1** and **2**, expectedly exhibit largely spectral blue shift and higher intensity both in PL and EL. Meanwhile, the carbazole appendage of complexes **2** and **4** do not significantly altering their PL performances in comparison with **1** and **3**, respectively, but have a modest increase in their EL efficiency in multilayer organic light-emitting diodes (OLEDs). Moreover, the OLED with **4** as light emitting material has the highest current efficiency (CE_{max}) of 27.2 cd/A and the maximum external quantum efficiency (EQE_{max}) of 8.7%.

Introduction

Multilayer OLEDs have attracted considerable attention for decades due to their huge application potentials in flat-panel displays and lighting devices[1-3]. One of the most important components is the luminescent dopant which dramatically determines the emission colour and the efficiency of the device[4-6]. Therefore, strongly emissive materials which harness both triplet and singlet excitons in device operation are indispensable in the fabrication of highly efficient OLEDs[7]. There are two types of materials can fully utilize the excitons: phosphorescent materials[8] and thermally-activated delayed fluorescent (TADF) materials[9, 10]. The most studied and used phosphors for OLEDs to date are emissive phosphorescent complexes of iridium[11-13] and other heavy transition metals[14, 15]. However, the natural resources of these metals are very limited, and they are usually highly expensive. Under this situation, it is demanding to find alternative materials with reliable resources and affordable cost. The possible solutions to lower the cost of the dopants are the application of environment benign and cost advantage TADF materials which based on copper[16] and carbon[17].

With promising electroluminescent properties, the emissive Cu(I) complexes have caused much attention and have been extensively studied as dopants for use in OLEDs[5, 18-21]. Over the last decade, many cuprous TADF materials exhibiting excellent electroluminescence performance comparable to the iridium counterparts have been found[22-27]. As dopants, there are two requirements needed to be satisfied to have highly efficient OLEDs. One is the highly photoluminescence efficiency, which, for cuprous complex, is mainly determined by the steric effect of ligands[28-31]. For them, the ligands with strong enough steric

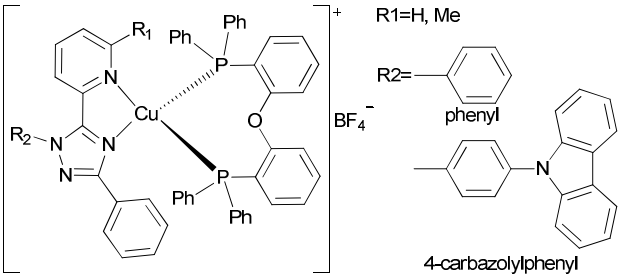

Fig. 1 Molecular structures of **1**–**4**.

hindrance can effectively suppress their geometry distortion which suppress non-radiative deactivation process in the exited state. The other is the higher utilization rate of excitons (caused by charge recombination and available to light) which can be facilitated through optimizing energy levels between charge transfer layers. It is noticed that introduction of electro- donating or withdrawing substituent groups at the ligands, because of their hole injection or electron transmission behaviors, partly improve the efficiency of the devices[32-34]. The incorporation of electron rich carbazole group into the complexes can boost the hole injection and transportation properties of OLEDs. This is the reason why compounds containing carbazole group are the most studied hole-transfer materials and are widely used as host materials for dopants immobilization[35, 36]. For the solution processed OLEDs, the hole-transfer layers were difficult to be optimized because the requirements for insoluble solvents among the various layers[4]. Recently, the carbazole group had been

View Article Online
DOI: 10.1039/C5DT01108F

appended to noble metal complexes and the efficiency of the solution processed OLEDs based on these complexes had been modestly improved[37, 38]. For the OLEDs using cationic cuprous complexes as dopants, because these complexes could hardly be sublimated, almost all of them were prepared by solution process. Therefore, coupling the carbazole groups to them potentially facilitates the efficiency of the OLEDs. However, the reports about carbazole groups which are coupled to emissive Cu(I) complexes are very rare[18, 39, 40].

In this work, four novel mononuclear cationic Cu(I) complexes (**1**–**4**) featuring functional 2-(5-phenyl-2*H*-1,2,4-triazol-3-yl)pyridine had been designed and synthesized (Fig. 1). Their photo- and electro-luminescent behaviours have been carefully studied. For **3** and **4**, methyl group was introduced to pyridine ring to block the geometry distortion in the excited state which, expectedly, lead to largely emission spectral blue shift and improve their PL and EL efficiency. Moreover, **2** and **4** with carbazole appendage show a modest increase (about 1.3 times) in device efficiency compared to **1** and **3**, respectively. The device based on **4** show high efficiency with CE_{max} of 27.2 cd/A and EQE_{max} of 8.7% while **3** had the CE_{max} of 21.4 cd/A and EQE_{max} of 6.7%.

Results and discussion

Synthesis and characterization

The diimine ligands 2-(5-phenyl-2-phenyl-2*H*-1,2,4-triazol-3-yl)pyridine (phtz), 2-(5-(4-carbazolyl)phenyl-2-phenyl-2*H*-1,2,4-triazol-3-yl)pyridine (phtzcz), 2-(5-phenyl-2-phenyl-2*H*-1,2,4-triazol-3-yl)-6-methylpyridine (mphtz), 2-(5-(4-carbazolyl)phenyl-2-phenyl-2*H*-1,2,4-triazol-3-yl)-6-methylpyridine (mphtzcz) were synthesized with similar procedures to the literature[41]. The cationic cuprous complexes $[Cu(phtz)(POP)]BF_4$ (**1**), $[Cu(phtzcz)(POP)]BF_4$, (**2**), $[Cu(mphtz)(POP)]BF_4$ (**3**) and $[Cu(mphtzcz)(POP)]BF_4$ (**4**) were obtained from the reaction of the precursors of $[Cu(POP)]BF_4$ and equivalent of corresponding diimine ligand. Spectroscopic pure products of these complexes were obtained by layering diethyl ether on the top of the CH_2Cl_2 solution of them and drying at 200 ºC under nitrogen. These compounds have high stability in the air no matter in the solid state or in the solutions of common organic solvents, such as methylene chloride and chloroform, presumably due to the bulky and ridge coordination environment of the cuprous ion. They were characterized by ^1H NMR, ^{31}P NMR, thermal analysis and elemental analysis.

The single crystals suitable for X-ray diffraction were prepared by slowly diffusion diethyl ether to the CH_2Cl_2 solution of these complexes. The ORTEP diagrams of them are displayed in Fig. 2. Highly distorted tetrahedral coordination for these cuprous complexes were observed with N–Cu–N and P–Cu–P angles in the range of 79.27º–80.70º and 114.12–118.27º (similar to values

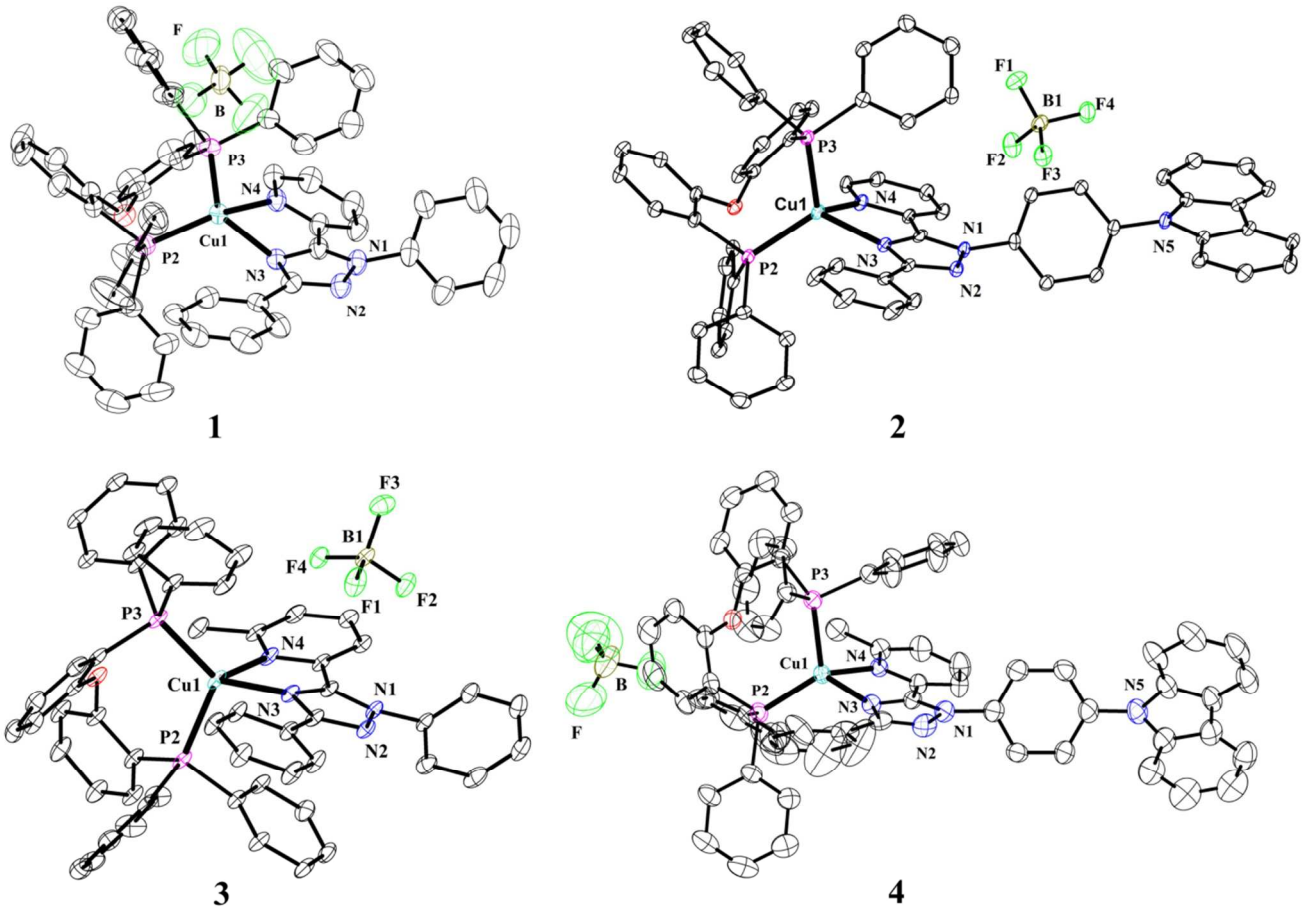

Fig. 2 ORTEP diagrams of **1**–**4** with thermal ellipsoids at 30% probability level. Solvent molecules and hydrogen have been omitted for clarity. Selected bond angles are N3–Cu1–N4 79.27(16), 79.60(11), 80.70(12) and 80.62(15) for **1**–**4** respectively; P2-Cu1-P3 114.12(6), 114.18(4), 116.29(4) and 118.27(5) for **1**–**4** respectively.

Dynamic Article Links ▶
View Article Online
DOI: 10.1039/C5DT01108F

Cite this: DOI: 10.1039/c0xx00000x

www.rsc.org/xxxxxx

ARTICLE TYPE

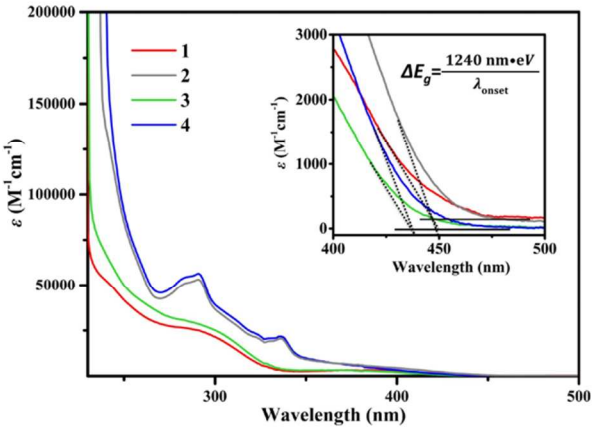

Fig. 3 Absorption spectra in CH_2Cl_2 of **1** (red), **2** (grey), **3** (green) and **4** (blue). The inset is the onsets of absorption spectra.

of previous reports[39, 42, 43]). Obviously, the methyl unit in the pyridine ring act as a steric hindrance group because of their enlarged N3–Cu–N4 and P2–Cu–P3 angles (> 1°) for **3** and **4** compared to **1** and **2**, which probably minimize the distortion that occurs in the excited state. Meanwhile, the steric influence of the substituent moiety on N1 seems negligible.

Photophysical properties

Absorption spectra in dichloromethane for complexes **1**–**4** are shown in Figure 3. As typical four coordinated $Cu(N,N)(P,P)^+$ complexes with a diimine and a biphosphine chelating ligands[42, 44], the absorption bands for them in the UV region (< 350 nm) are dominated by the spin allowed intraligand π-π^* transitions of the diimine ligands and the POP ligands. At longer wavelength, from 350 nm to 420 nm, ligand-ligand charge transfer and metal-ligand charge-transfer (MLCT) states are usually attributed. The broad band centered at about 385 nm for **1** and **3** are typical for ^{1}MLCT from d orbitals on the copper metal center to empty π^* orbitals localized on the diimine ligands. For compounds **2** and **4**, the transitions below 350 nm are more intense in comparison with the bands of compounds **1** and **3** which are caused by the intraligand charge transitions of carbazole appendage at diimine ligand[39]. The onset wavelength of absorption spectrum is usually used to estimate the energy gap (ΔE_g) between HOMO and LUMO of complex. As shown in inset of Fig. 3, complexes **1** and **2** have the same ΔE_g (2.77ev), while **3** and **4** have the same ΔE_g (2.85ev), suggesting the methyl moiety at pyridine ring increases the energy gap of the frontier orbitals and the carbazole appendage have negligible charge contribution to these orbitals (Table S4). Moreover, the larger ΔE_g values for **3** and **4**, compared to **1** and **2**, respectively, potentially suppress the thermal population

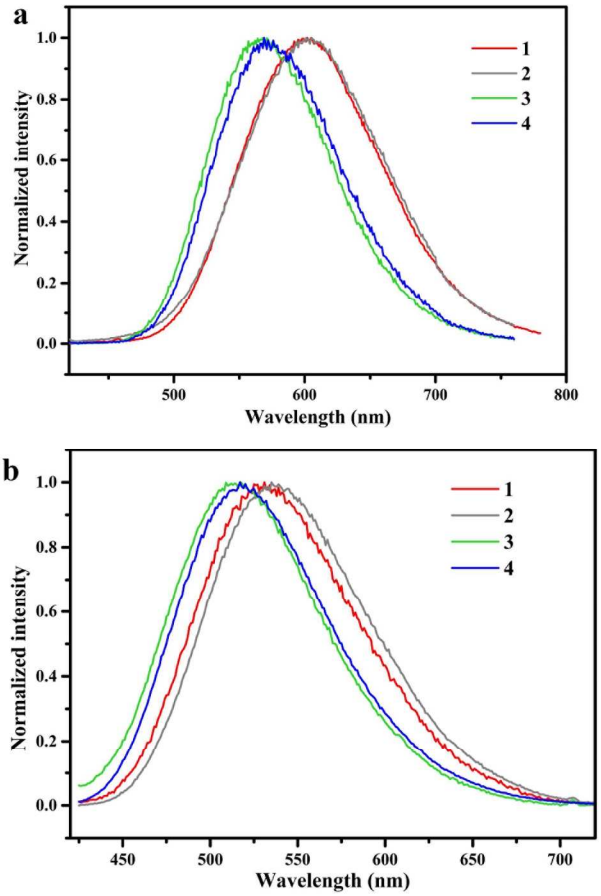

Fig. 4 (**a**) Emission spectra of **1**–**4** in CH_2Cl_2. (**b**) Emission spectra of **1**–**4** in PMMA.

Table 1 Photophysical properties of **1**–**4** in the solvent and PMMA film.

	Solvent				PMMA film				
	λ_{abs}(nm) ($\varepsilon\times10^{-3}M^{-1}$ cm^{-1})	λ_{em}(nm)	$\tau_{ave}{}^a$(μs)	Φ^b(%)	λ_{em}(nm)	$\tau_{ave}{}^a$(μs)	Φ^b(%)	k_r (s^{-1})	k_{nr} (s^{-1})
1	284(26), 374(3.3)	601	1.7	3	532	7.7	16	2.1×10^4	1.1×10^5
2	291(53), 337(21), 374(6.6)	601	1.9	5	537	6.3	14	2.2×10^4	1.4×10^5
3	284(31), 374(3.3)	567	1.4	19	516	7.5	48	6.4×10^4	6.9×10^4
4	291(56), 337(22), 377(5.9)	569	1.6	16	517	6.8	37	5.4×10^4	9.3×10^4

[a] Emission decay time (monoexponential fit, error ±5%). [b] photoluminescence quantum yield (error ± 7%) at 298 K;.

View Article Online
DOI: 10.1039/C5DT01108F

Cite this: DOI: 10.1039/c0xx00000x

www.rsc.org/xxxxxx

ARTICLE TYPE

radiationless transition more effectively (energy gap law[45]) and lead to emission spectral blue shift.

At room temperature, all complexes were found to be strongly emissive. Their photophysical properties were studied in solid state, in CH_2Cl_2 and in PMMA film. Their spectra in the solid state are shown in supporting information (Fig. S4 and table S3) and the spectra in the solvent and thin film are shown in Fig. 4. Independent of the matrix, their emission spectra are broad and unstructured, which is consistent with the charge transfer nature of the emission [35]. The photoluminescence quantum yields (Φ_{PL}) and calculated radiative decay rate (k_r) and the nonradiative decay rate (k_{nr}) from Φ_{PL} and τ_{ave} based on the solvent and thin film are listed in table 1. For all of these complexes, blue-shifting and increasing quantum yield of the emissions were observed as the

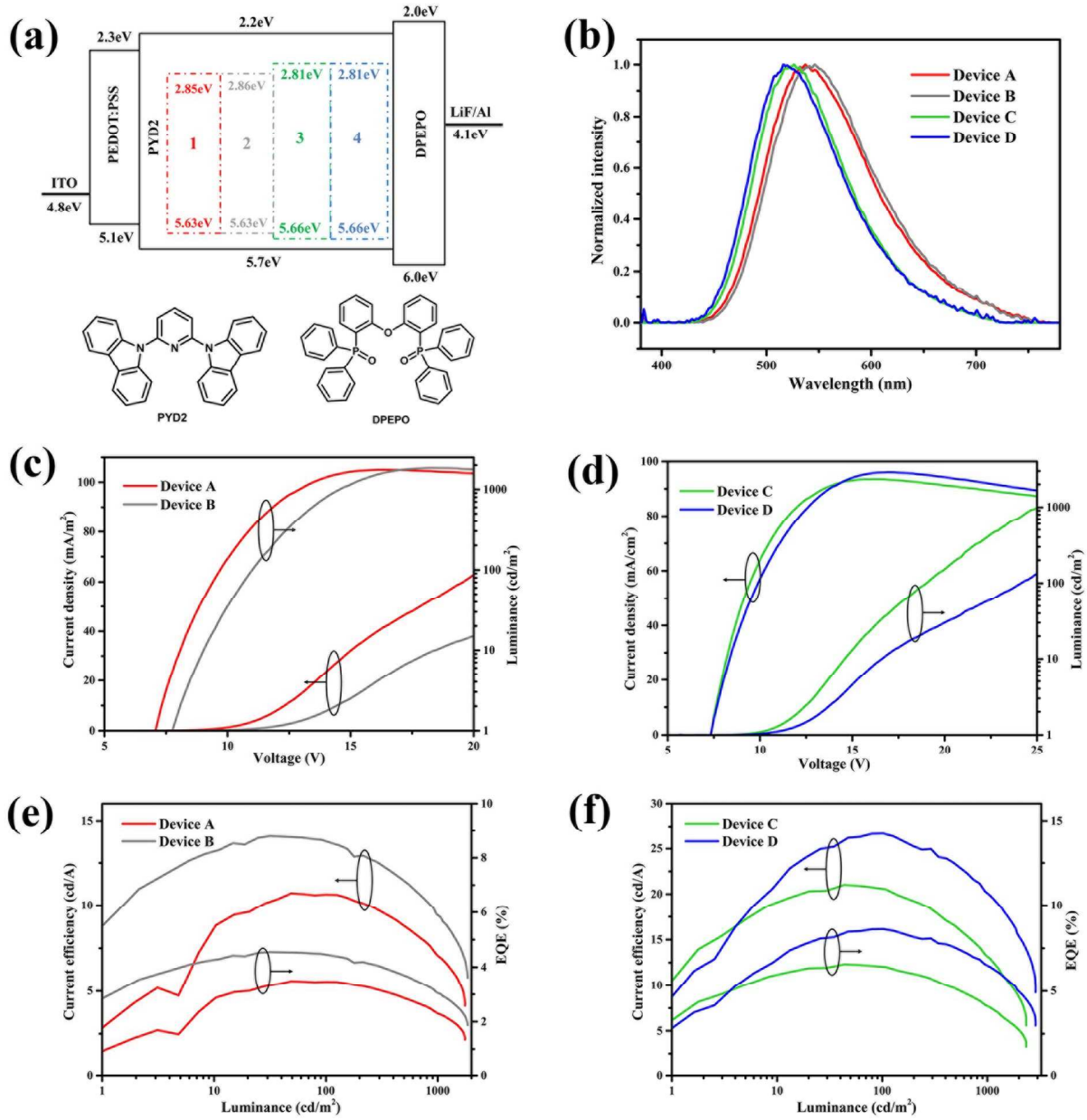

Fig. 5 (a) Device configuration and relate molecular structures of PYD2 and DPEPO. (b) Electroluminescence spectra of devices A–D containing **1**–**4** respectively. (c), (d) Plots of Current density and luminance *vs* voltage for devices. (e), (f) Plots of CE and EQE *vs* luminescence for devices.

Dynamic Article Links ►
View Article Online
DOI: 10.1039/C5DT01108F

Cite this: DOI: 10.1039/c0xx00000x

www.rsc.org/xxxxxx

ARTICLE TYPE

Table 2 Electroluminescence characteristics of OLEDs.

Device	Dopant	$V_{turn\text{-}on}$ (V)	Luminance (cd/A)[a]	CE (cd/A)[a]	EQE (%)[a]	λ_{max} (nm)[b]
A	**1**	7.1	1750	10.7	3.5	537 (0.31, 0.41)
B	**2**	7.8	1850	14.1	4.6	546 (0.32, 0.51)
C	**3**	7.3	2339	21.4	6.7	526 (0.25, 0.45)
D	**4**	7.3	2893	27.1	8.7	516 (0.24, 0.42)

[a] Maximum values of the devices. [b] Data were collected at 10 V; CIE coordinates shown in parentheses..

matrix rigidity increases from the solvent to the thin film. This observation is common for emissive cuprous complexes because of the existence of geometric rearrangement from the tetrahedral-like ground state (d^{10}) to the flattened excited state (d^9) upon MLCT excitation [46]. With an increasing of the matrix rigidity, the freedom for changes of the molecular geometries upon MLCT excitation is decreased, and the above-mentioned distortions can be suppressed [47].

Herein, the discussions focus on their emission properties in the thin film because these properties are similar to that in devices. As shown in Table 1, in the PMMA film, complex **3** has the highest Φ_{PL} and k_r. The k_r for **1** is smaller than that for **3** by about two times, while the k_{nr} for **1** is larger than that for **3** by about 160%. Similar results were found for complexes **2** and **4**. The larger k_r for the complexes **3** and **4** which lead to higher Φ_{PL} of them ascribe to the methyl group at pyridine ring that act as steric hindrance group effectively suppressing the geometry distortion in the excited state. Furthermore, the emission spectra of **1** and **2** are very similar, **3** and **4** are similar too. It seems to suggest that the carbazole groups on N1, unlike at the *o*-position of coordination nitrogen[39], have limited influence on the steric and electronic character of these complexes.

Electroluminescence performances

All of these complexes were chosen to fabricate OLED (A, B, C, D) with the configuration: ITO/PEDOT:PSS (40 nm)/5 wt% of **1**, **2**, **3** or **4**:PYD2 (2,6-bis(N-carbazolyl)pyridine, 30 nm)/DPEPO (bis[2-(di-(phenyl)phosphino)-phenyl]ether oxide, 50 nm)/LiF (0.7 nm)/Al (100 nm) (where ITO is indium tinoxide, PEDOT:PSS is poly (3, 4-ethylenedioxythiophene)–poly(styrenesulfonic acid). In this configuration, PYD2 and DPEPO act as hole transmission and electron transmission materials, respectively. The HOMOs of these complexes were estimated from onset of their positive potential cyclic voltammetry curves while the values of LUMOs were calculated by adding ΔE_g to the values of HOMOs. The hole-injection and emitting layers were prepared by spin coating, and the remaining layers were deposited by thermal evaporation. The configuration and the EL characteristics of OLED are shown in Fig. 5 and table 2. The EL spectra of these devices are in good agreement with their spectra in the PMMA film. Additionally, there are no additional shoulder of PYD2, indicating effective exciton recombination and confinement in the emitting layer.

The EL performances of these complexes are in consistent with their PL performances which are mainly determined by the coordination steric effect of the ligands too. As aforementioned, their geometry distortion were suppressed by the methyl group at pyrindine ring, thus complexes **3** and **4** show higher device efficiency with excellent CE_{max} of 21.4 cd/A and 27.2 cd/A, EQE_{max} of 6.7% and 8.8%, respectively, than **1** (10.7 cd/A, 3.5%) and **2** (14.1 cd/A, 4.6%). According to this, the EQE_{max} of the devices based on complexes **2** and **4** with carbazole appendage approximate 1.3 times higher than that of **1** and **3** respectively. It is noteworthy mention that **2** and **4** show slightly poorer PL efficiency both in the PMMA film and solution than **1** and **3**, respectively. Taken together, these data suggest that the carbazole group for this series of complexes benefits the utilization of the excitons that caused by charge recombination in device operation which slightly facilitate device efficiency.

Conclusions

In this work, we designed four new emissive cuprous complexes containing functional 2-(5-Phenyl-2*H*-1,2,4-triazol-3-yl)pyridine diimine ligands. Complexes **3** and **4** with steric methyl group at pyridine ring expectedly show largely emission spectral blue-shift and improved efficiency both in PL and EL than **1** and **2** which further convince the importance of space steric hindrance for emitting properties. Meanwhile, complexes **2** and **4** with carbazole appendage show limited spectral variation and slightly higher device efficiency as compared to **1** and **3**, respectively. The results suggest that the device efficiency based on this kind of complexes are also mainly determined by the steric effect of substituent group and can be further elevated by the electron rich carbazole group while it act as hole carrier.

Experimental

General procedures

Reagents and solvents were purchased from commercial sources and used without further purification. All reactions were performed under N_2 atmosphere using standard Schlenk techniques unless specified. The complex $[Cu(CH_3CN)_4]BF_4$ and the two materials 2,6-bis(N-carbazolyl)pyridine (PYD2) and

View Article Online
DOI: 10.1039/C5DT01108F

bis[2-(di-(phenyl)phosphino)-phenyl]ether oxide (DPEPO) used in device fabrications were prepared according to literature procedures[48, 49]. ^{1}H NMR and ^{31}P NMR spectra were recorded on a Bruker Avance III 400 MHz NMR spectrometer. Elemental analyses (C, H, N) were carried out with an Elementar Vario EL III elemental analyzer.

Ligands preparation

The ancillary diimine ligands phtz, phtzcz, mphtz, mphtzcz were synthesized from the precursors 2-(5-phenyl-2*H*-1,2,4-triazol-3-yl)pyridine (HPhtz) and 6-Me-2-(5-phenyl-2*H*-1,2,4-triazol-3-yl)pyridine (MePhtz) according to reported procedures[41] (Fig. S1). The mixture of 1eq. of 6-R-picolinonitrile (R= H, Methyl) and 0.3 eq. of sodium in anhydrous methanol was refluxed for 3 h and then 1 eq. of benzoyl hydrazine was added. The solution was refluxed till yellow solid precipitated. After filtration and drying, the solid was added to glycol solution and heated to reflux for 3 h, then cooled to room temperature and stand overnight. Colourless crystal (HPhtz or MePhtz) was obtained after the removal of solvent.

HPhtz or MePhtz (2.07 mmol), 1, 10-phenanthroline (0.827 mmol), copper(I) iodide (0.413 mmol), caesium carbonate (4.13 mmol), 2.07mmol iodobenzene for phtz or mphtz, 9-(4-iodophenyl)-9*H*-carbazole for phtzcz or mphtzcz were dissolved in dry DMF (10 mL). The mixture was stirred vigorously for 1 h at room temperature and then heated to 100 ºC under nitrogen for another 36 h. At room temperature, the residue was filtrated. The liquid phase was extracted with CH_2Cl_2 (3 × 30 mL) and washed with water, subsequently dried with anhydrous sodium sulphate. After the removal of solvent under vacuum, the crude product was purified by column chromatography on silica gel with ethyl acetate/petroleum ether.

Cuprous complexes preparation

A mixture of $[Cu(CH_3CN)_4]BF_4$ (1.0 mmol) and POP(1.0 mmol) in CH_2Cl_2 (10 mL) was stirred at room temperature for 1 h, then the corresponding diimine ligand (1.0 mmol) was added. The reaction mixture was stirred for another 1 h. The spectroscopic pure products were obtained through diffuse diethyl ether into the solution of these complexes and dried 0.5 h at 90 ºC. According to the TGA, the samples used for Elemental analyses (C, H, N) and NMR were dried 5 h at 200 ºC. The 1H NMR diagrams suggest that there are solvents residual for **4** (about 0.2 eq. of dichloromethane and 0.2 eq. of diethyl ether) (Appendix). The content of solvents is in consistent with the weight loss (2.9%) from 220 to 320 ºC (TGA).

[Cu(phtz)(POP)]BF_4 **(1).** ^{1}H NMR (400 MHz $CDCl_3$): δ 8.29 (d, 1H), 7.98(d, 2H), 7.81(t, 1H), 7.71(m, 3H), 7.5–7.27(m, 10H), 7.25–6.9(m, 25H). ^{31}P NMR: δ -11.99(s). Anal. Calcd for $CuC_{55}H_{42}ON_4P_2BF_4$: C, 66.91; N, 5.68; H, 4.29. Found: C, 66.73; N, 5.41; H, 4.18.

[Cu(phtzcz)(POP)]BF_4 (**2**). ^{1}H NMR (400 MHz $CDCl_3$): δ 8.35 (d, 1H), 8.16 (d, 2H), 7.92–8.02 (m, 5H), 7.71 (d, 2H), 7.61 (d, 2H), 7.28–7.53 (m, 12H), 6.9–7.25 (m, 21H). ^{31}P NMR: δ -11.71(s). Anal. Calcd for $CuC_{67}H_{49}ON_5P_2BF_4$: C, 69.83; N, 6.08; H, 4.29. Found: C, 69.47; N, 6.03; H, 3.89.

[Cu(mphtz)(POP)]BF_4 (**3**). ^{1}H NMR (400 MHz $CDCl_3$): δ 7.80 (d, 2H), 7.71–7.64 (m, 3H), 7.40–7.28 (m, 10H), 7.25–6.91 (m, 26H), 2.01 (s, 3H). ^{31}P NMR: δ -13.45 (s). Anal. Calcd for $CuC_{56}H_{44}ON_4P_2BF_4$: C, 67.17; N, 5.60; H, 4.43. Found: C, 67.21; N, 5.38; H, 4.25.

[Cu(mphtzcz)(POP)]BF_4•0.2(CH_2Cl_2)•0.2(diethyl ether) (**4**). ^{1}H NMR (400 MHz $CDCl_3$): δ 8.15 (d, 2H), 7.96 (t, 1H), 7.90 (d, 2H), 7.84 (d, 2H) 7.64–7.58 (dd, 4H), 7.52–7.45 (m, 4H), 7.38–7.28 (m, 10H) 6.90–7.25 (m, 23H), 5.3 (s, 0.4H), 3.48 (dd, 0.8H), 2.05 (s, 3H), 1.21 (t, 1.2H). ^{31}P NMR: δ -13.43 (s). Anal. Calcd for $CuC_{69}H_{53.4}O_{1.2}N_5P_2BF_4$: C, 69.16; N, 5.84; H, 4.49. Found: C, 69.05; N, 5.81; H, 4.24.

X-ray Crystallographic Analysis

Diffraction data of complexes **1** and **4** were collected on a Saturn724 CCD Rigaku Mercury and a diffractometer equipped with graphite-monochromated Mo Kα radiation (λ = 0.71073 Å), respectively. Diffraction data of complexes **2** and **3** were collected on a SuperNova, Dual, Cu at zero, Atlas diffractometer equipped with graphite-monochromated Cu Kα radiation (λ =1.54184 Å). Structures were solved by direct methods and refined by full-matrix least-squares methods with SHELXL-97 program package. Hydrogen atoms were added in idealized positions. All nonhydrogen atoms were refined anisotropically. Details of crystal and structure refinement are listed in Table S1, selected bond length and angles are displayed in Table S2. Owing to a serious disorder problem at data collection, there is an alert level A for **1** attributed to the serious disorder solvents. The solvent molecules could not be crystallographically defined successfully. But the TGA and NMR analysis show that there are dichloromethane and diethyl ether molecules in the compound **1**. CCDC: 1034650–1034653 contain the supplementary crystallographic data of complexes **1**–**4,** respectively.

Thermogravimetric analysis (TGA) experiments

TGAs were done on a NETZSCH STA 449C Jupiter thermogravimetric analyzer in flowing nitrogen with the sample heated in an Al_2O_3 crucible at a heating rate of 10 $Kmin^{-1}$ (Figure S3). The samples used for experiments have been dried at 90ºC for 30 min. The weight loss 4%, 1.6% for complexes **1** and **3** under 200ºC belong to the release of residual solvents. The solvents loss (2.9%) from 220 to 320 ºC for complex **4** attribute to 0.2 eq. of dichloromethane and diethyl ether. The decomposition temperatures for these four complexes are up to 350ºC (Fig. S2).

Electrochemical Measurement

Cyclic voltammetry was performed in a gastight single-compartment three-electrode cell with a BAS Epsilon Electrochemical Analyzer at room temperature. A glassy carbon disk and a platinum wire were selected as the working and auxiliary electrodes, respectively. The reference electrode was Ag/Ag^+ (0.1 M of $AgNO_3$ in acetonitrile). The CV measurements were carried out in anhydrous and nitrogen-saturated CH_2Cl_2 solutions with 0.1 M n-tetrabutylammonium perchlorate (TBAP) and 2.0 mM cuprous complex. The ferrocenium/ferrocene couple was used as an internal standard. (Fig. S3)

Photophysical Measurements

The solution samples for the photophysical studies were carefully degassed ($[Ru(bpy)_3]^{2+}$ in degassed water was selected as reference for the PL quantum yields of them[50]). The film samples

View Article Online
DOI: 10.1039/C5DT01108F

were prepared by spin-coating a mixture of the cuprous complex and poly(methyl methacrylate) (PMMA) in distilled CH_2Cl_2 onto a quartz glass slide and dried under vacuum at 50 °C for 2 h before measurements. The powder samples were obtained by drying the crystals at 90 °C for 0.5 h and measured without further treatment. UV−vis absorption spectra were recorded with a Perkin-Elmer Lambda 45 UV/vis spectrophotometer. Photoluminescence spectra at room temperature were recorded on a HORIBA Jobin-Yvon FluoroMax-4 spectrometer. The lifetimes were measured by the time-correlated single-photon counting (TCSPC) upgrade on the FluoroMax-4 spectrometer with a FluoroHub module. The thin film and powder PL quantum yields were defined as the number of photons emitted per photon absorbed by the systems and measured by FluoroMax-4 equipped with an integrating sphere.

Device Fabrication and Characterization

The hole-blocking material bis[2-(di(phenyl)phosphino)-phenyl]ether oxide (DPEPO) was purified by sublimation after recrystallization. Poly(3,4-ethylene dioxythiophene):poly(styrene sulfonic acid) (PEDOT:PSS) was purchased from Heraeus and filtered through 0.22 mm filter before use. Other materials used in the device fabrication were purchased and used without further purification. A 40 nm thick PEDOT:PSS film was first spin-coated (at 3000 rpm) on a pre-cleaned ITO-glass substrate and then dried at 140 °C for 20 min. The emitting layer was then overlaid with spin-coating (at 1500 rpm) of CH_2Cl_2 solution with host and dopant (0.5 mg of **1**, **2**, **3** or **4** and 9.5 mg of PYD2 dissolved in 1.8 mL CH_2Cl_2). The film was then dried under vacuum for 1 h at room temperature. Subsequently, 50 nm of DPEPO, 0.8 nm of LiF and 100 nm of Al were deposited under pressure less than 4×10^{-4} Pa. The electroluminescence (EL) spectra were recorded on a HORIBA Jobin-Yvon FluoroMax-4 spectrometer. Current density−voltage−luminance (*J*−*V*−*L*) curves of these devices were recorded on a Keithley 2400/2000 source meter and a calibrated silicon photodiode at room temperature in air. All measurements on the devices were carried out at room temperature. The calculated energy for these complexes is listed in table S4.

Acknowledgements

This work was supported by the 973 key program of the Chinese Ministry of Science and Technology (MOST) (2012CB821705), the Chinese Academy of Sciences (KJCX2-YW-319, KJCX2-EW-H01), the National Natural Science Foundation of China (21373221, 21221001, 91122027, 51172232) and the Natural Science Foundation of Fujian Province (2006L2005).

Notes and references

[a] *Key Laboratory of Design and Assembly of Functional Nanostructures, Fujian Institute of Research on the Structure of Matter, Chinese Academy of Sciences; Fuzhou, Fujian 350002, China. Fax: +86-591-8370-5794. E-mail: czlu@fjirsm.ac.cn.*

[b] *Fujian Provincial Key Laboratory of Nanomaterials, Fujian Institute of Research on the Structure of Matter, Chinese Academy of Sciences, Fuzhou, Fujian 350002, China.*

[c] *Graduate University of Chinese Academy of Sciences, Beijing 100049, China.*

† Electronic Supplementary Information (ESI) available: Supplementary computational and experimental data. CCDC number 1034650-1034653. For ESI and crystallographic data in CIF or other electronic format see DOI: 10.1039/b000000x/

1. S. Reineke, F. Lindner, G. Schwartz, N. Seidler, K. Walzer, B. Lüssem and K. Leo, *Nature*, 2009, **459**, 234–238.
2. Y. Sun, N. C. Giebink, H. Kanno, B. Ma, M. E. Thompson and S. R. Forrest, *Nature*, 2006, **440**, 908–912.
3. M. Segal, M. Singh, K. Rivoire, S. Difley, T. Van Voorhis and M. A. Baldo, *Nat Mater*, 2007, **6**, 374–378.
4. L. W. Qisheng Zhang, *Adv. Mater.*, 2004, **16**, 432–435.
5. M. Osawa, M. Hoshino, M. Hashimoto, I. Kawata, S. Igawa and M. Yashima, *Dalton Trans*, 2014, DOI: 10.1039/c4dt02853h.
6. L. Ying, C. L. Ho, H. Wu, Y. Cao and W. Y. Wong, *Adv. Mater.*, 2014, **26**, 2459–2473.
7. S. Difley, D. Beljonne and T. Van Voorhis, *J. Am. Chem. Soc.*, 2008, **130**, 3420–3427.
8. H. Xu, R. Chen, Q. Sun, W. Lai, Q. Su, W. Huang and X. Liu, *Chem. Soc. Rev.*, 2014, **43**, 3259–3302.
9. Q. Zhang, B. Li, S. Huang, H. Nomura, H. Tanaka and C. Adachi, *Nat Photonic*, 2014, **8**, 326–332.
10. T. Hofbeck, U. Monkowius and H. Yersin, *J. Am. Chem. Soc.*, 2015, **137**, 399–404.
11. S. Soman, J. C. Manton, J. L. Inglis, Y. Halpin, B. Twamley, E. Otten, W. R. Browne, L. De Cola, J. G. Vos and M. T. Pryce, *Chem Commun*, 2014, **50**, 6461–6463.
12. C. Murawski, P. Liehm, K. Leo and M. C. Gather, *Adv. Funct. Mater.*, 2014, **24**, 1117–1124.
13. Y. C. Zhu, L. Zhou, H. Y. Li, Q. L. Xu, M. Y. Teng, Y. X. Zheng, J. L. Zuo, H. J. Zhang and X. Z. You, *Adv. Mater.*, 2011, **23**, 4041–4046.
14. M. C. Tang, D. P. Tsang, Y. C. Wong, M. Y. Chan, K. M. Wong and V. W. Yam, *J. Am. Chem. Soc.*, 2014, **136**, 17861–17868.
15. G. Li, T. Fleetham and J. Li, *Adv. Mater.*, 2014, **26**, 2931–2936.
16. D. Volz, M. Wallesch, C. Fléchon, M. Danz, A. Verma, J. M. Navarro, D. M. Zink, S. Bräse and T. Baumann, *Green Chem.*, 2015, **4**, 1988–2011.
17. S. Hirata, Y. Sakai, K. Masui, H. Tanaka, S. Y. Lee, H. Nomura, N. Nakamura, M. Yasumatsu, H. Nakanotani, Q. Zhang, K. Shizu, H. Miyazaki and C. Adachi, *Nat Mater*, 2015, **14**, 330–336.
18. Z. W. Liu, J. Qiu, F. Wei, J. Q. Wang, X. C. Liu, M. G. Helander, S. Rodney, Z. B. Wang, Z. Q. Bian, Z. H. Lu, M. E. Thompson and C. H. Huang, *Chem. Mater.*, 2014, **26**, 2368–2373.
19. M. Hashimoto, S. Igawa, M. Yashima, I. Kawata, M. Hoshino and M. Osawa, *J. Am. Chem. Soc.*, 2011, **133**, 10348–10351.
20. J. C. Deaton, S. C. Switalski, D. Y. Kondakov, R. H. Young, T. D. Pawlik, D. J. Giesen, S. B. Harkins, A. J. Miller, S. F. Mickenberg and J. C. Peters, *J. Am. Chem. Soc.*, 2010, **132**, 9499–9508.
21. F. Dumur, *Org. Electron.*, 2015, **21**, 27–39.
22. M. Osawa, *Chem Commun*, 2014, **50**, 1801–1803.
23. M. J. Leitl, V. A. Krylova, P. I. Djurovich, M. E. Thompson and H. Yersin, *J. Am. Chem. Soc.*, 2014, **136**, 16032–16038.
24. R. Czerwieniec, J. Yu and H. Yersin, *Inorg. Chem.*, 2011, **50**, 8293–8301.
25. M. Osawa, I. Kawata, R. Ishii, S. Igawa, M. Hashimoto and M. Hoshino, *J. Mater. Chem. C.*, 2013, **1**, 4375–4379.
26. B. P. Rand, H. Yersin, R. Czerwieniec, A. Hupfer, C. Adachi and V. van Elsbergen, *spie*, 2012, **8435**, 84350801–84350810.
27. D. Volz, Y. Chen, M. Wallesch, R. Liu, C. Flechon, D. M. Zink, J. Friedrichs, H. Flugge, R. Steininger, J. Gottlicher, C. Heske, L. Weinhardt, S. Brase, F. So and T. Baumann, *Adv. Mater.*, 2015, **15**, 2538–2543.
28. V. Kalsani, M. Schmittel, A. Listorti, G. Accorsi and N. Armaroli, *Inorg. Chem.*, 2006, **45**, 2061–2067.
29. D. G. Cuttell, S.-M. Kuang, P. E. Fanwick, D. R. McMillin and R. A. Walton, *J. Am. Chem. Soc.*, 2002, **124**, 6–7.
30. Q. Zhang, J. Chen, X. Y. Wu, X. L. Chen, R. Yu and C. Z. Lu, *Dalton Trans*, 2015, **44**, 6706–6710.
31. Q. Zhang, X.-L. Chen, J. Chen, X.-Y. Wu, R.-M. Yu and C.-Z. Lu, *RSC Adv.*, 2015, **43**, 34424–34431.

View Article Online
DOI: 10.1039/C5DT01108F

32. T. Giridhar, C. Saravanan, W. Cho, Y. G. Park, J. Y. Lee and S. H. Jin, *Chem Commun*, 2014, **50**, 4000–4002.
33. C. Fan, Y. Li, C. Yang, H. Wu, J. Qin and Y. Cao, *Chem. Mater.*, 2012, **24**, 4581–4587.
34. B. Krummacher, M. K. Mathai, V. E. Choong, S. A. Choulis, F. So and A. Winnacker, *Org. Electron.*, 2006, **7**, 313–318.
35. X.-L. Chen, R. Yu, Q.-K. Zhang, L.-J. Zhou, X.-Y. Wu, Q. Zhang and C.-Z. Lu, *Chem. Mater.*, 2013, **25**, 3910–3920.
36. Y. C. Chen, G. S. Huang, C. C. Hsiao and S. A. Chen, *J. Am. Chem. Soc.*, 2006, **128**, 8549–8558.
37. Y. You and S. Y. Park, *Dalton Tans.*, 2009, 1267–1217.
38. H. Xu, D. H. Yu, L. L. Liu, P. F. Yan, L. W. Jia, G. M. Li and Z. Y. Yue, *J. Phys. Chem. B*, 2010, **114**, 141–150.
39. X.-L. Chen, C.-S. Lin, X.-Y. Wu, R. Yu, T. Teng, Q.-K. Zhang, Q. Zhang, W.-B. Yang and C.-Z. Lu, *J. Mater. Chem. C.*, 2015, **3**, 1187–1195.
40. Z. Liu, M. F. Qayyum, C. Wu, M. T. Whited, P. I. Djurovich, K. O. Hodgson, B. Hedman, E. I. Solomon and M. E. Thompson, *J. Am. Chem. Soc.*, 2011, **133**, 3700–3703.
41. G.-G. Shan, H.-B. Li, D.-X. Zhu, Z.-M. Su and Y. Liao, *J. Mater. Chem.*, 2012, **22**, 12736–12739.
42. S. Igawa, M. Hashimoto, I. Kawata, M. Yashima, M. Hoshino and M. Osawa, *J. Mater. Chem. C.*, 2013, **1**, 542–510.
43. L. Bergmann, J. Friedrichs, M. Mydlak, T. Baumann, M. Nieger and S. Brase, *Chem Commun*, 2013, **49**, 6501–6503.
44. J. L. Chen, X. F. Cao, J. Y. Wang, L. H. He, Z. Y. Liu, H. R. Wen and Z. N. Chen, *Inorg. Chem.*, 2013, **52**, 9727–9740.
45. J. V. Caspar, E. M. Kober, B. P. Sullivan and T. J. Meyer, *J. Am. Chem. Soc.*, 1982, **104**, 630–632.
46. M. Iwamura, S. Takeuchi and T. Tahara, *J. Am. Chem. Soc.*, 2007, **129**, 5248–5256.
47. N. Armaroli, G. Accorsi, F. Cardinali and A. Listorti, *Top. Curr. Chem.*, 2007, **280**, 69–115.
48. H. Xu, L. H. Wang, X. H. Zhu, K. Yin, G. Y. Zhong, X. Y. Hou and W. Huang, *J. Phys. Chem. B*, 2006, **110**, 3023–3029.
49. G. J. Kubas, *Inorg. Syn.*, 1979, **XIX**, 90–93.
50. J. Vanhouten and R. J. Watts, *J. Am. Chem. Soc.*, 1976, **98**, 4853–4858.

View Article Online
DOI: 10.1039/C5DT01108F

Graphical Abstract

Steric methyl group at emissive cuprous complexes largely increases both the PL and EL efficiency while the carbazole appendage modestly improves the EL efficiency. So **4** show the highest efficiency with CE_{max} of 27.1 cd/A and EQE_{max} of 8.7%.